A Diagnostic Study of Pacific Basin Circulation Regimes as Determined from Extratropical Cyclone Tracks

JOHN R. ANDERSON

Department of Meteorology, University of Wisconsin, Madison, Wisconsin

JOHN R. GYAKUM

Department of Meteorology, McGill University, Montreal, Quebec, Canada

(Manuscript received 1 November 1988, in final form 11 May 1989)

ABSTRACT

The interannual and intraseasonal track variability of cold season extratropical cyclones in the Pacific basin is examined using an 8 year cyclone track dataset. An EOF technique incorporating VARIMAX rotation in time is used to objectively describe the regime nature of the variations. Based upon this analysis we conclude that the cyclone behavior can be classified into six major regime types, corresponding to the positive and negative amplitude excursions of each of the first three rotated EOFs. Each of these rotated EOFs explains approximately equal fractions of the total variance. A study of the cyclone tracks for individual extreme periods confirms the existence of times where each of these patterns dominate. The average 500 mb height fields for these extreme periods have been examined and are generally consistent with the cyclone track anomalies. The resultant regime description shows strong interannual variability; however, there appears to be little obvious correlation with the ENSO signal, suggesting that a significant fraction of the interannual variability may be generated within the middle and high latitudes.

1. Introduction

The low frequency behavior of the midlatitude atmosphere is a topic which has been extensively studied over the past twenty years. These studies have focused on time scales ranging from 10–15 day "blocking" events to interannual fluctuations. Most of these studies have used midtroposphere variables such as 500 mb height fields. In this study, we present a complementary analysis, namely, the exploration of the low frequency variability of the frequency and tracks of midlatitude surface cyclones. We have examined the cyclone behavior in a Pacific basin domain which extends from 20° to 70°N, 120°E to 120°W. This region was chosen since it is a region frequently associated with strong variability on both blocking and interannual time scales.

It is well known that variations in the midtropospheric flow have a profound impact on the generation and tracks of midlatitude cyclones. In fact, the name "blocking" was coined to describe the tendency for long-lived circulation anomalies to prevent the normal movement of storms across the Atlantic basin, thus resulting in profound changes in European weather patterns. Early descriptions of blocking activity appear in Elliot (1949), Namias and Clapp (1949) and Rex (1950). More recently objective classifications of these phenomena have been proposed and studied by Dole (1986), who has defined and characterized a class of "persistent anomaly" events in terms of the 500 mb height fields. In addition to the investigation of blocking events themselves, other investigators, such as White and Clark (1975) have noted a relationship between interannual variability such as that associated with the ENSO phenomena and the propensity toward blocking. Following the extreme 1976/77 winter in the eastern United States, much effort has been expended on exploring this relationship. Recently Lau (1988) has investigated the behavior of cyclone activity using a proxy variable for the storm tracks consisting of the monthly mean rms amplitudes of 500 mb height fluctuations in a synoptic time scale frequency band. The relationship of this proxy variable to traditional synoptic storm tracks has been discussed by Wallace et al. (1988). We will compare our results with those of the Lau study to assess the effects of our use of actual surface cyclone positions and our higher time resolution, which can represent the shorter blocking time scales.

For this study we have chosen to create a cyclone based circulation variable, namely a space- and time-smoothed cyclone track density function; and then to analyze the interannual and intraannual variability of

Corresponding author address: Dr. John R. Anderson, Dept. of Meteorology, University of Wisconsin, 1225 West Dayton Street, Madison, WI 53706.

this field with the goal of producing a description of the variability in Pacific cyclone activity that can be compared with other circulation indices.

The methodology that we will follow is to create the track density field and then characterize the nonseasonal variability of this field using a standard EOF analysis. The outputs of the EOF analysis will then be processed in order to produce a better description of individual regime patterns. Here we have chosen to perform this task using an EOF rotation which simplifies the time series associated with each spatial pattern. That is, the rotation is chosen so as to assign a single pattern to each time as much as possible, as opposed to the original EOF analysis where sums of several EOFs are usually important for the description of the anomaly field at a given time.

The results of the rotated EOF analysis are then used to define a classification of the 8 year time period into regimes where each regime is characterized by a strong positive or negative value for one of the EOF time series. Finally, we will go back and examine the cyclone tracks for some of these extreme periods to verify that the classification does indeed provide a useful description of the cyclone variability.

2. Construction of cyclone density fields

The dataset used in this study is an 8 year cold season compilation of Pacific Basin cyclones. The dataset covers the months of October to March for the period from 1975/76 to 1982/83. The cyclone positions were produced by transcribing the positions of analyzed storms from the twice daily NMC final surface analyses for the period. A more detailed description of the dataset is given in Gyakum et al. (1989).

The first step in the analysis is the construction of a cyclone track density field, $C(\mathbf{x}, t)$. This field is designed to provide a description of the storm tracks on time scales of two weeks and longer rather than to describe the movement of individual storms. This is accomplished by evaluating (1a) on a 5 deg latitude by 5 deg longitude grid with 1 day time resolution

$$C(\mathbf{x}, t) = \sum_j W(\mathbf{x} - \mathbf{x}_j, t - t_j) \qquad (1a)$$

where

$$W(\Delta X, \Delta t) = \cos^2 \frac{|\Delta X|}{S_x} \cos^2 \frac{|\Delta t|}{S_t} \qquad (1b)$$

when $|\Delta X|/S_x$ and $|\Delta t|/S_t$ are less than $\pi/2$; otherwise $W = 0$.

Here $\mathbf{x}_j$ is the position of the jth cyclone observation which is valid at time t_j. The summation is taken over all of the cyclone observations in the dataset. The $W(\Delta X, \Delta t)$ is a weighting function which defines the space and time extent of the smoothing used to create C. The space and time resolution of the analysis is determined by the parameters S_x and S_t, which are set to $14/\pi$ deg of latitude and $28/\pi$ days, respectively. This is roughly equivalent in resolution to a bin counting procedure using a ±3.5 degree box with ±7 day time resolution. However, the use of the weighting function allows the somewhat better rejection of the high frequency spatial and temporal fluctuations.

Once the cyclone track density field has been created, a nonseasonal anomaly field is then computed. This anomaly field is generated by subtracting a climatology based on the least squares fit of the first two (annual and semiannual) seasonal harmonics to the 8 year dataset at each point on the 5 × 5 deg grid. Plots showing the spatial distribution of the field means and the standard deviations of the anomaly field appear in Fig. 1.

3. EOF analysis with time rotation

The next step in our analysis is the computation of an EOF representation of the anomaly field. This computation was performed with daily time resolution on the analysis grid using an iterative singular decomposition technique where a first guess field is repeatedly projected though the dataset in time and then space until convergence is reached. Once each EOF has been found, the variance associated with that EOF is removed using the Grahm–Schmidt reorthonormalization technique and the procedure is repeated. Although no correlation or covariance matrices are actually computed, since we do not normalize the data by standard deviation, this procedure is equivalent to finding the eigenvalues of the covariance matrix. The first three EOFs explain 14.66%, 11.66%, and 9.20% of the variance respectively. The space fields and associated time series for these EOFs appear in Figs. 2 and 3.

In an attempt to assess the statistical significance of our results, we have performed a Monte Carlo experiment where 50 control experiments were computed and compared with our analysis. The dataset for each control experiment consisted of randomly scrambling the starting dates for each of the cyclones in the dataset to prevent real correlation between tracks of different storms. When this experiment was performed, the first three EOFs from our analysis explained a greater residual variance than any of their counterparts in the 50 control calculations, indicating a substantial degree of significance when compared to the null hypothesis that each storm track could be considered to be an unrelated event.

The description of the field provided by the EOF analysis provides an approximate Mth order representation, C^M, for the field in terms of a linear space–time separation of variables as shown in (2). The EOF problem is closed by requiring minimum squared error for any truncation order M up to the number of degrees of freedom in the initial dataset

$$C^M(\mathbf{x}, t) = \sum_{j=1}^{M} X_j(\mathbf{x}) T_j(t). \qquad (2)$$

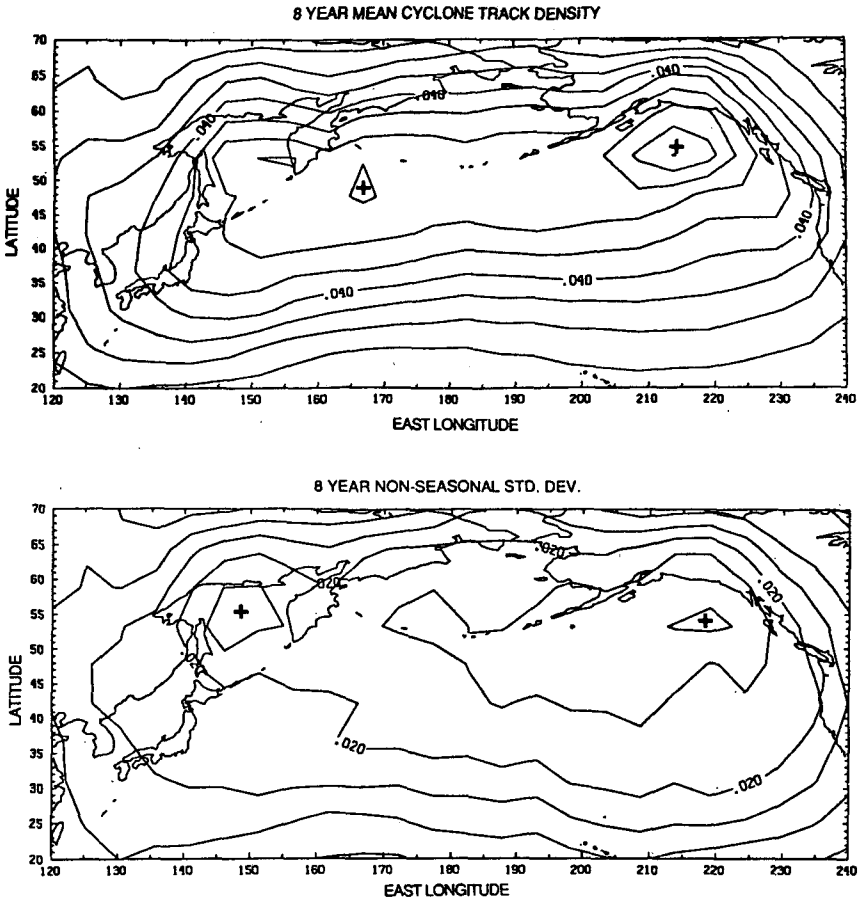

FIG. 1. Mean and standard deviation of cyclone track density field. Contour intervals are 0.01 and 0.005 cyclones/day/5 × 5 deg, respectively.

An unfortunate consequence of this optimality property is the tendency to generate EOF patterns that rarely appear in their pure form but appear instead in combination with other EOFs to represent the fields. An example of this effect can be noted in the EOF 2 pattern, which does not seem to correspond to a reasonable set of anomalous cyclone tracks. This can be confirmed by noting that the time series of EOF 2 amplitude is rarely large by itself. In most cases, one of the other EOFs also has a substantial amplitude and together they describe the behavior for that time. In this study we are interested in determining the structure of cyclone "regimes," meaning typical cyclone behavior patterns such as blocking events which actually appear in more or less pure form.

One approach for simplifying the interpretation of an EOF analysis, is the technique of factor rotation which has been used in meteorological applications by Horel (1981) and others. A description of the rotation procedure can be found in the text of Cureton and D'Agostino (1983) and a review of various rotation methods for meteorological problems can be found in Richman and Lamb (1985). When performing an EOF rotation, one must first choose a value for the truncation, M. Once this value is chosen, (2) is then replaced with an analogous expression involving new space and time factors, X' and T', that are formed by computing linear combinations of the original EOF factors (3).

$$C^M(\mathbf{x}, t) = \sum_{j=1}^{M} X'_j(\mathbf{x}) T'_j(t) \tag{3a}$$

$$X'_j(\mathbf{x}) = \sum_{i=1}^{M} \alpha_{i,j} X_i(\mathbf{x}) \tag{3b}$$

$$T'_j(t) = \sum_{i=1}^{M} \beta_{i,j} T(t). \tag{3c}$$

Here, the α and β represent the rotation matrices, which are determined by optimizing some form of "simplicity" parameter. Traditionally, the rotation is made so as to simplify the spatial structure, X', of the factors; however, here we have adopted the alternate strategy of performing the rotation so as to simplify the temporal structure, T'. The particular "simplicity" measure

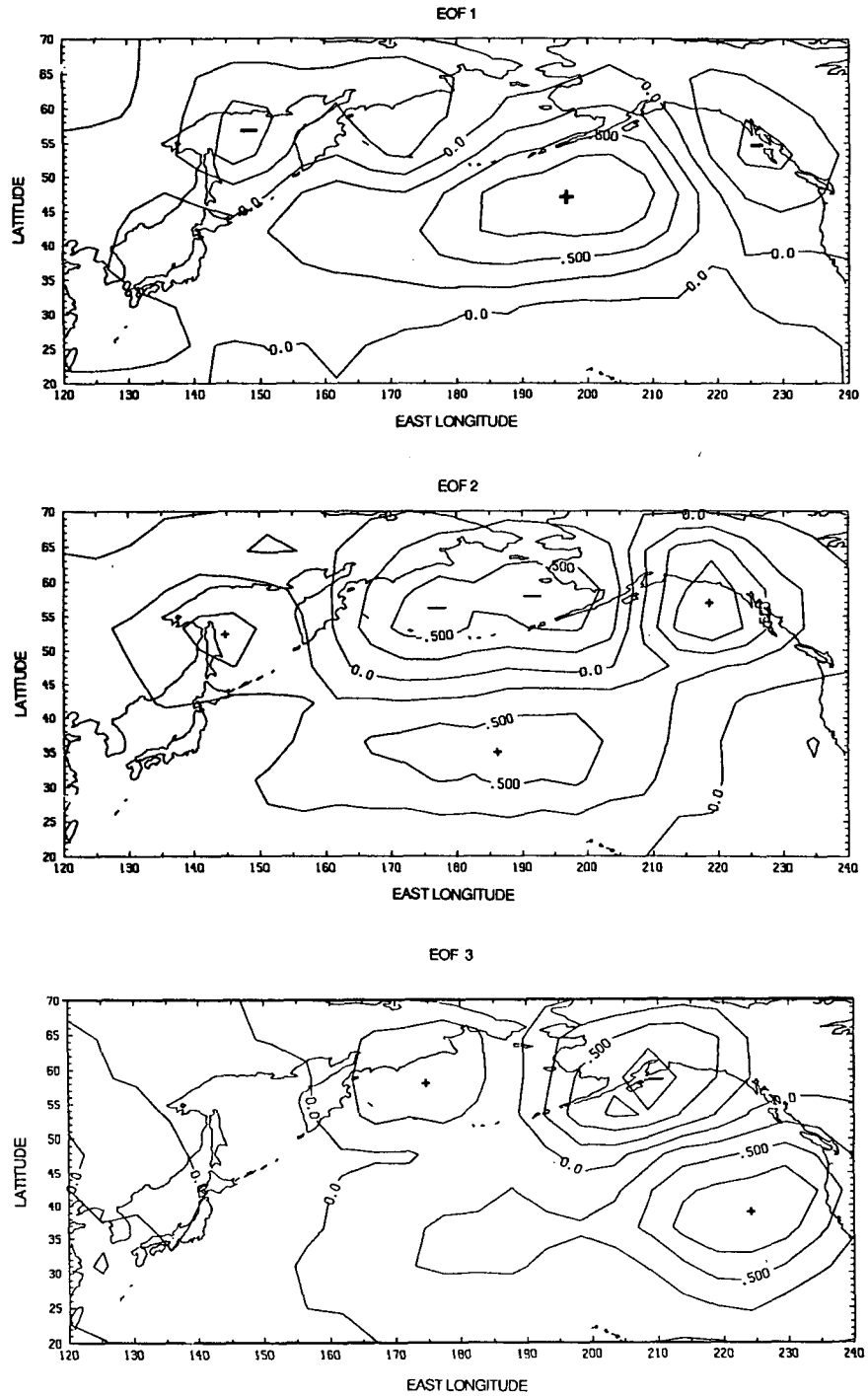

FIG. 2. The EOF space fields, $X(\mathbf{x})$, of the first three unrotated EOFs.

which we have chosen is a VARIMAX measure, V which is given by

$$V = \sum_{t} \sum_{j=1}^{M} (T'_j(t))^4 - \sum_{t} \sum_{j=1}^{M} (T'_j(t))^2. \quad (4)$$

The time rotation coefficients, b, are determined by maximizing V under the constraint that b represents an orthogonal rotation operator. Due to the dependence of V on the fourth power of the time series, the result of this maximization is to choose the time series such that individual times are represented as much as

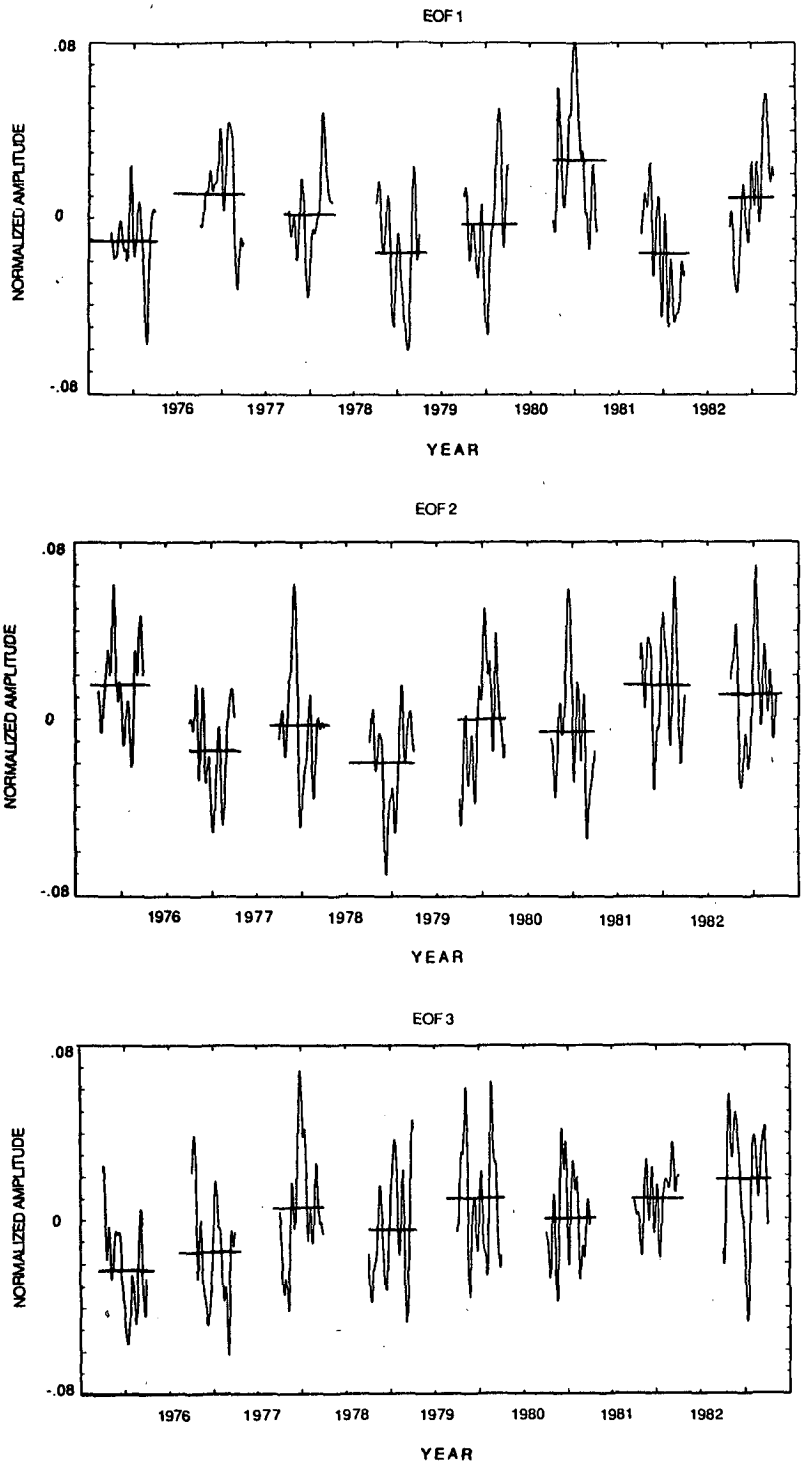

FIG. 3. The EOF time fields, $T(t)$, of the first three unrotated EOFs.

possible by one of the rotated EOFs rather than a combination of several. In this way various time periods can be classified into regimes based on which of the EOF patterns dominated the expansion (3a) for that particular time.

One of the difficulties in performing such an analysis is the issue of choosing a truncation value for the rotation. This problem has so far resisted efforts aimed at formulating a robust, objective method. A recent discussion of the problem appears in O'Lenic and Liv-

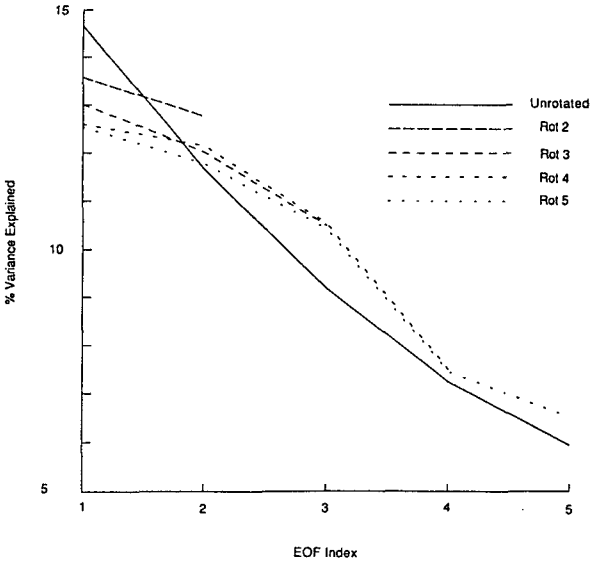

FIG. 4. Explained variance for the first five unrotated EOFs and the results of the time domain VARIMAX rotation for $M = 2, 3, 4,$ and 5.

ezey (1988). Fortunately, for our purposes, this particular analysis appears to have a natural truncation point and the results are nearly insensitive to the choice. A plot of the variance explained by the first five EOFs in the unrotated case, and the variance for rotations with M taken to be 2, 3, 4, and 5 appears in Fig. 4. For rotations with $M = 3$, 4, or 5, the first three rotated EOFs explain similar amounts of the variance followed by a substantial drop-off in explained variance by 4 and 5 for the $M = 4$ and $M = 5$ rotations. In addition, the space and time structures of the first three rotated EOFs are nearly identical for truncations of $M = 3$, 4, and 5. It seems that $M = 3$ represents a reasonable truncation point for the problem, implying that in some sense the anomalous periods can be described in terms of six regimes; each showing a strong positive or negative value for one of the three time series.

The time and space series associated with the $M = 3$ rotation appear in Figs. 5 and 6. The effect of the rotation on the time series is made readily apparent by comparing them with the unrotated case. All of the time series plots are normalized so that the squares of the values sum to 1; however, in each case, the rotated series show a stronger tendency toward large peak positive or negative values associated with the increased VARIMAX measure. In addition, the space fields and in particular, the EOF 2 field, now have a substantially more "physical" appearance consisting of a simple dipole structure which represents the northward or southward movement of the central cyclone track in contrast to the previous EOF 2 field which had three separate positive centers that did not appear to be well related. In the next section, we will demonstrate that these patterns are well correlated with the anomalous cyclone tracks during extreme periods and we will demonstrate using an independent dataset that the regimes are associated with appropriate 500 mb height anomaly fields. EOF 1 is nearly unchanged by the rotation, and the rotation has emphasized a more wavelike nature of EOF 3. It is important to realize that these changes in the spatial pattern were accomplished without any direct use of the spatial data during the rotation optimization.

4. Discussion of extreme period patterns

In this section, we will investigate the cyclone track behavior during the high amplitude periods of each of the rotated EOF time series. Using this technique, we will refer to periods where EOF 1 has a large positive amplitude as type 1+ cases, periods where EOF 1 has a large negative amplitude as 1− cases, and so on. We will examine the cyclone track behavior during six 30-day sample periods which exhibit consistently large positive and negative amplitudes in each of the three time series. These periods we have chosen consist of the largest amplitude cases where the anomaly is extended over the full 30 day period, or the longest possible anomaly if none extended that long.

In addition to the cyclone track patterns, we have also prepared plots of the 500 mb height and 500 mb height anomaly fields for the six extreme periods. These fields were constructed from the NMC 500 mb gridpoint analysis and were produced using the University of Washington compact disk distribution of this dataset (Mass et al. 1987). It should be pointed out that the plots of the cyclone tracks represent the actual cyclone tracks during a period and not the track anomalies. Therefore when comparing the track pictures to the EOF patterns, one needs to take the mean track density as depicted in Fig. 1a into account. Since the 500 mb patterns can be plotted as anomalies these fields can be compared directly with the EOF fields and provide a means for independent verification of our results since only the track data was used in selecting the extreme periods.

Our example of a 1+ type regime is the 30-day period from 15 January to 13 February 1977. The cyclone tracks for this period are shown in Fig. 7a. During this period, a very well defined zonal cyclone track maximum across the central Pacific leads to a collection of occluded cyclones near the Alaska peninsula and very few cyclone tracks successfully reaching the west coast of North America. The 500 mb means for this period (Figs. 7b and 7c) show a consistent pattern with a closed 500 mb low in the eastern and central Pacific with heights 214 m below normal and a West Coast ridge reaching 157 m above normal heights for this 30 day period.

The sample 1− regime is the period from 8 February to 10 March 1982. Here, Fig. 8a shows a split track pattern with well-defined cyclone tracks in the eastern

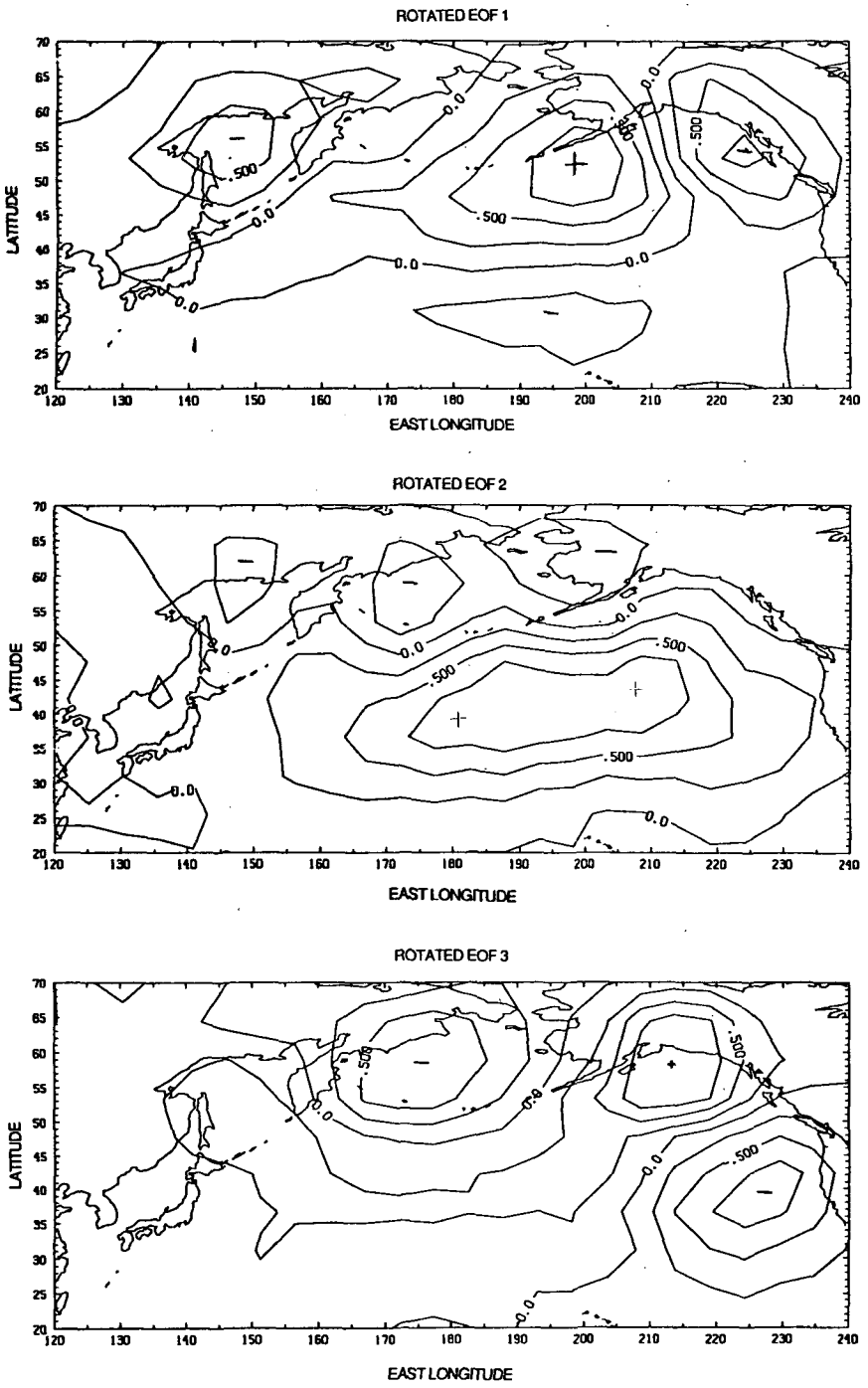

FIG. 5. The EOF space fields, $X'(\mathbf{x})$, of the first three EOFs for the $M = 3$ rotation.

and western parts of the Pacific basin, but very few storms traverse the central Pacific region. This agrees well with the strong (+195 m) central Pacific 500 mb ridge depicted in Figs. 8b and 8c.

The period from 2 December to 31 December 1980 is dominated by a 2+ type pattern. It shows a zonal, southern track across the entire basin with storms preceeding well east of the turning point seen in the 1+ cases (Fig. 9a), although the eastern ends of the tracks become rather diffuse. The 500 mb fields (Figs. 9b, c) are reminiscent of an "omega" block in the Central Pacific and show anomalously low heights from 20° to 40°N and generally high heights from 50° to 70°N.

The tracks during our 2− example period from 28

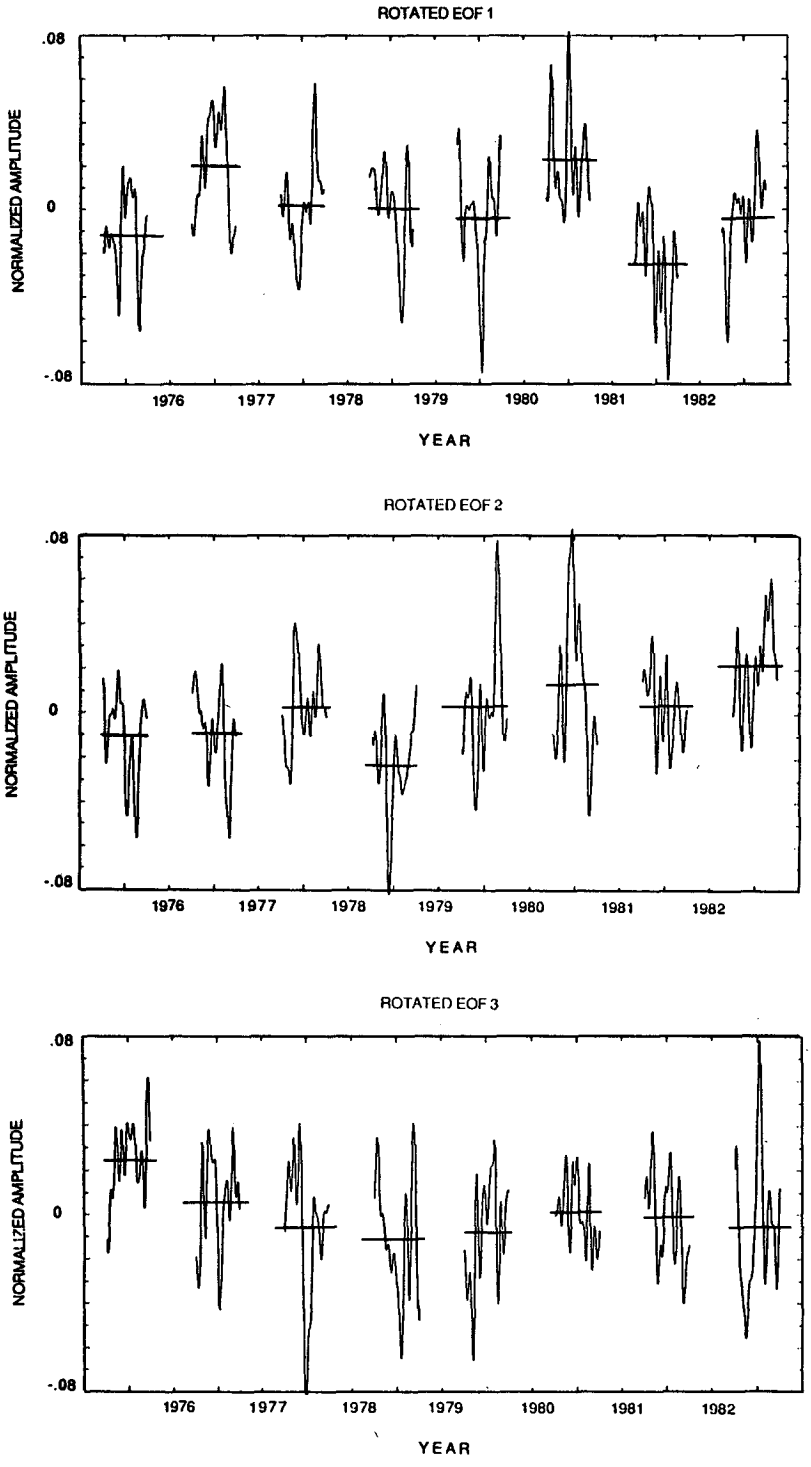

FIG. 6. The EOF time fields, $T'(t)$, of the first three EOFs for the $M = 3$ rotation.

November to 27 December 1978 are perhaps the most striking pattern during our study (Fig. 10a). Here we see an extremely well defined cyclone track that starts in the far eastern Pacific and extends northeast into the Bering Sea with most of the storms passing north of the Aleutians and almost no cyclone activity in the southeastern part of our domain. Again, the 500 mb fields (Figs. 10b, c) provide an independent verification of the cyclone track patterns exhibiting strong positive anomalies south of Alaska.

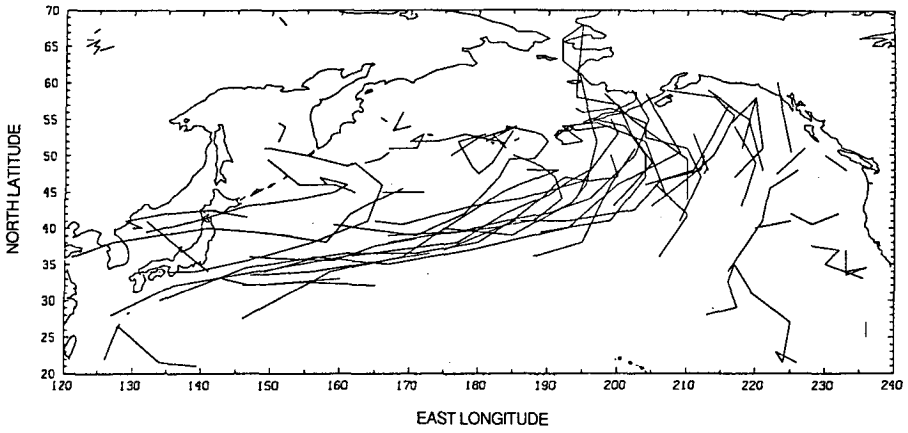

FIG. 7a. Cyclone tracks for 15 January 1977–13 February 1977: Type 1+ regime.

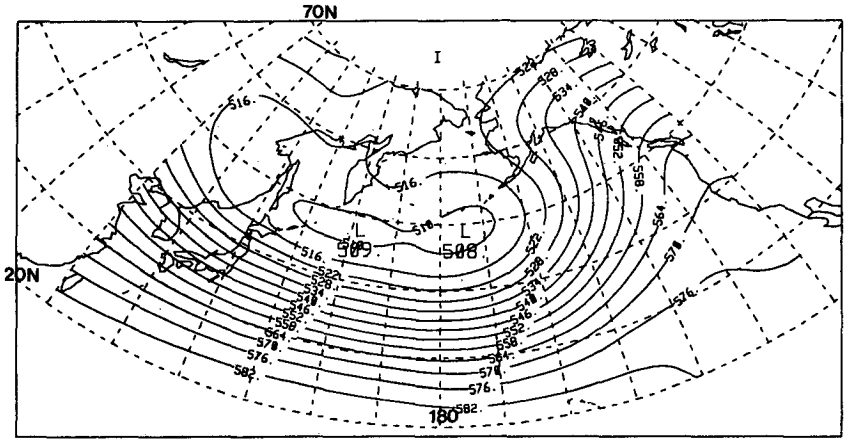

FIG. 7b. Composite field of 500 mb geopotential height for the period 15 January 1977–13 February 1977 at 1200 UTC: Type 1+ regime. The contour interval is 6 decameters.

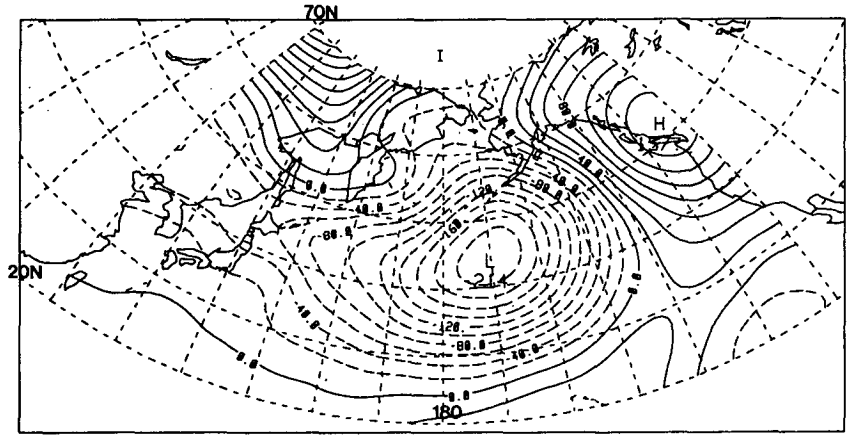

FIG. 7c. Composite field of 500 mb geopotential height anomalies for the period 15 January 1977–13 February 1977 at 1200 UTC: Type 1+ regime.

The patterns (Figs. 11a, b, and c) associated with a 3+ period of 22 December to 20 January 1983 resemble the 1+ pattern with an eastward shift of about 15 degrees of longitude. Note that this pattern differs from the 2+ pattern in that the central Pacific tracks are north of the 2+ tracks and show a well-defined turning

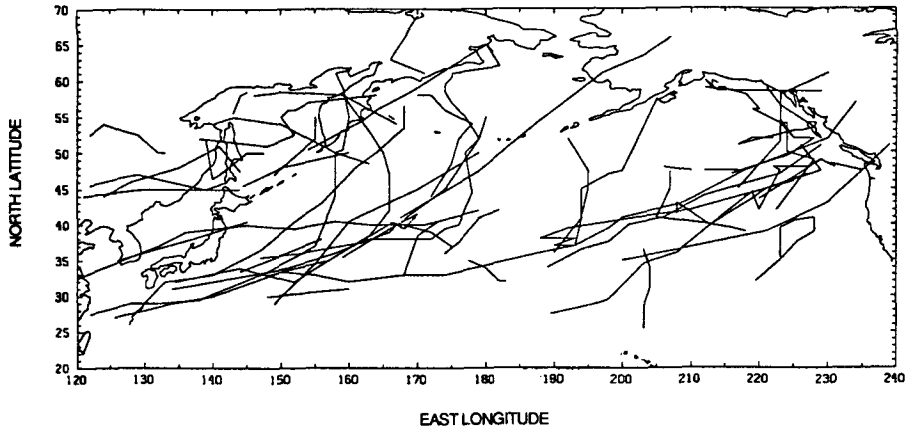

FIG. 8a. Cyclone tracks for 9 February 1982–10 March 1982: Type 1− regime.

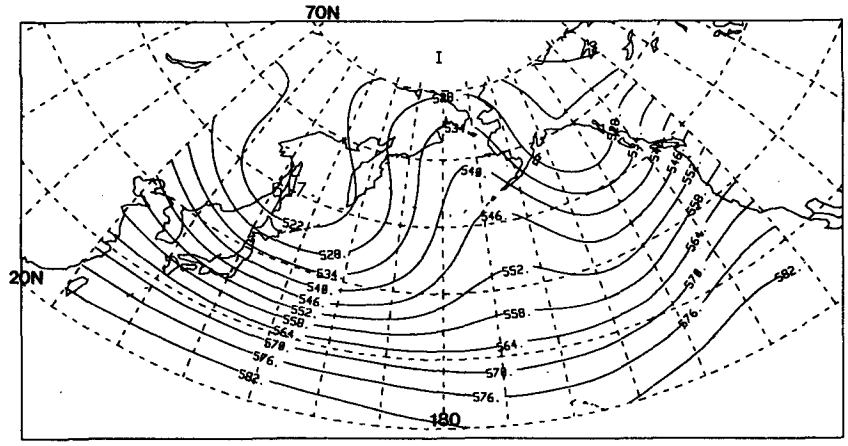

FIG. 8b. Composite field of 500 mb geopotential height for the period 9 February 1982–10 March 1982 at 1200 UTC: Type 1− regime. The contour interval is 6 decameters.

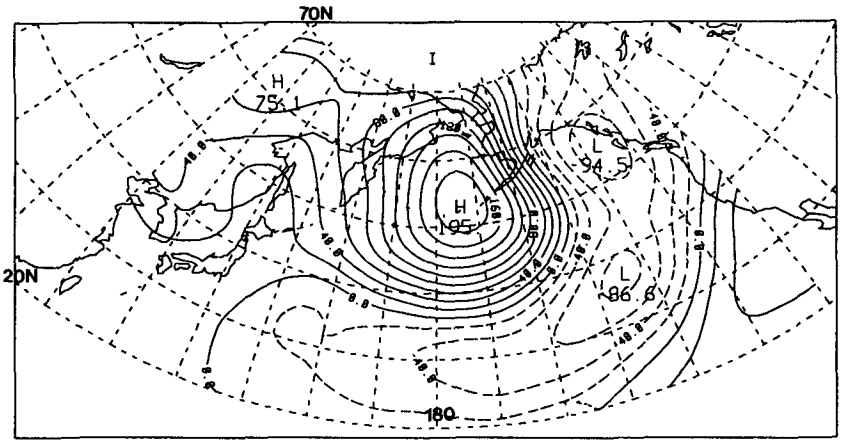

FIG. 8c. Composite field of 500 mb geopotential height anomalies for the period 9 February 1982–10 March 1982 at 1200 UTC: Type 1− regime.

point in the Gulf of Alaska, as opposed to the diffuse termination of the 2+ pattern.

The 3− regime depicted in the 19 December to 17 January 1978 example (Figs. 12a, b, and c) is similar to the split track pattern of the 1− example, but again shifted to the east. In contrast to the 1− pattern, the

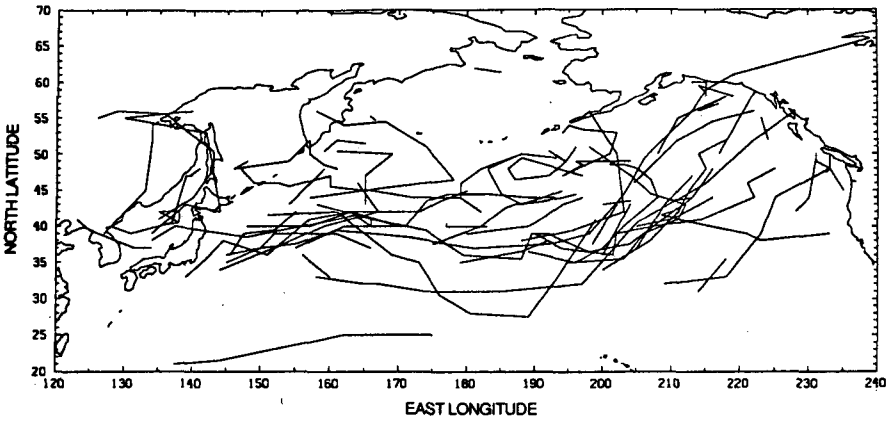

FIG. 9a. Cyclone tracks for 2 December 1980–31 December 1980: Type 2+ regime.

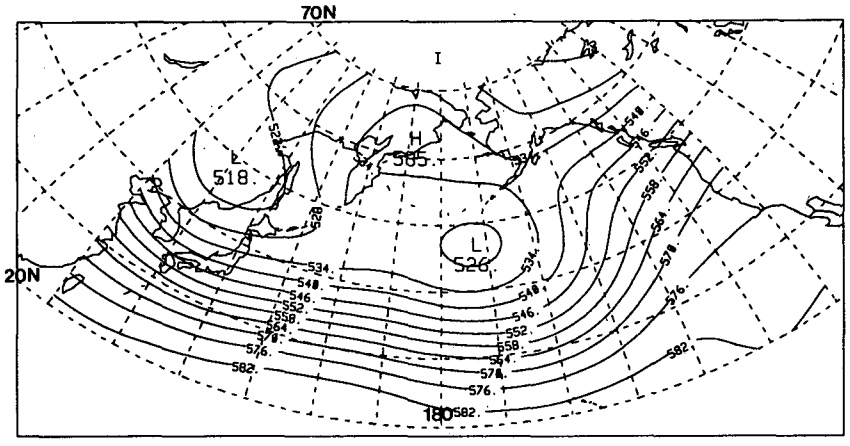

FIG. 9b. Composite field of 500 mb geopotential height for the period 2 December 1980–31 December 1980 at 1200 UTC: Type 2+ regime. The contour interval is 6 decameters.

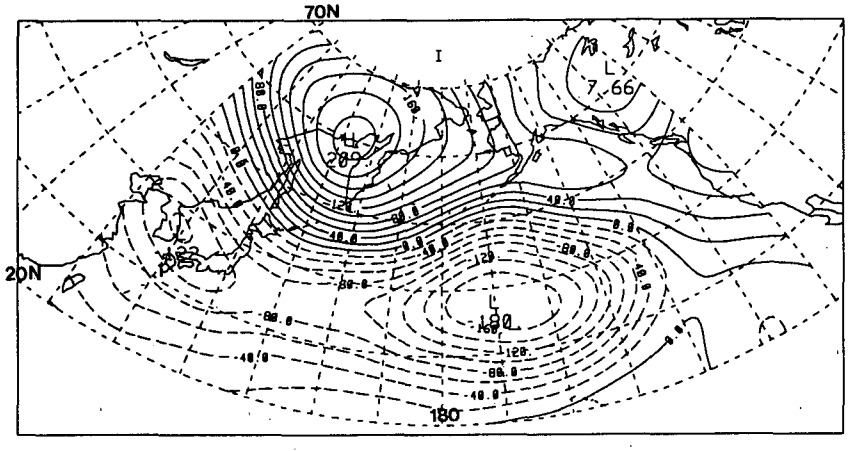

FIG. 9c. Composite field of 500 mb geopotential height anomalies for the period 2 December 1980–31 December 1980 at 1200 UTC: Type 2+ regime.

western branch now continues into the Bering Sea rather than curving into northeast Asia while the eastern branch hits the North American continent south of the eastern branch in the 1− example. This eastward shift is also apparent when comparing the 500 mb fields. The apparent similarity of the 1− and 3− fields

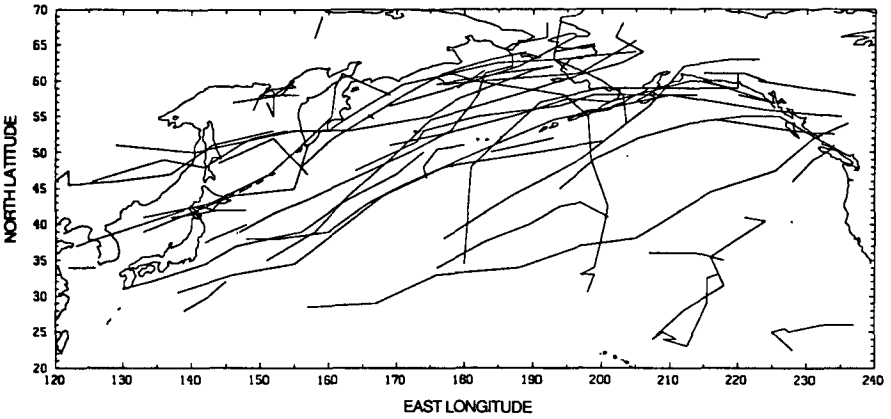

FIG. 10a. Cyclone tracks for 28 November 1978–27 December 1978: Type 2− regime.

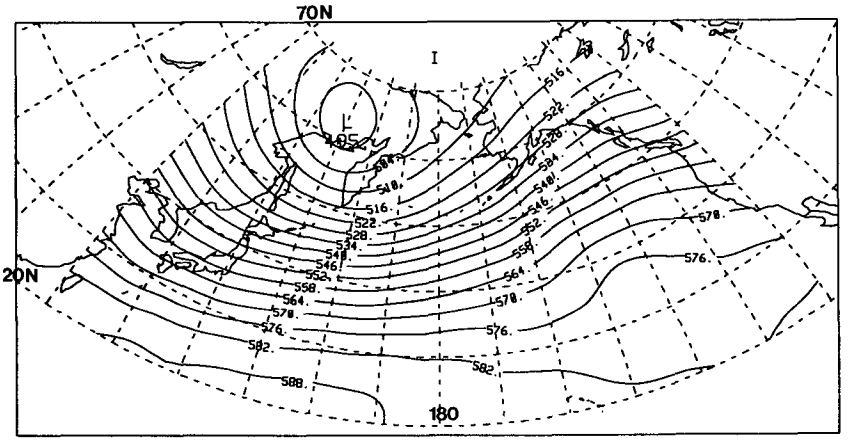

FIG. 10b. Composite field of 500 mb geopotential height for the period 28 November 1978–27 December 1978 at 1200 UTC: Type 2− regime. The contour interval is 6 decameters.

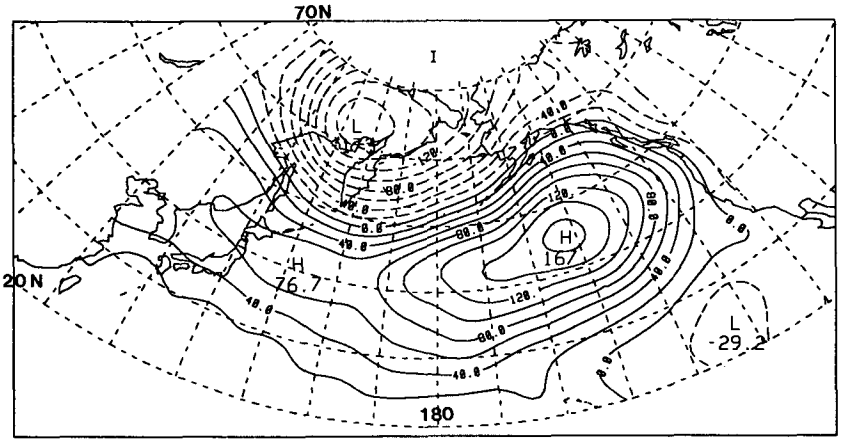

FIG. 10c. Composite field of 500 mb geopotential height anomalies for the period 28 November 1978–27 December 1978 at 1200 UTC: Type 2− regime.

is due in part to the fact that the EOFs have large amplitudes in only the final sections of the eastern and western Pacific cyclone tracks and the main portions of the tracks exhibit near climatological densities.

5. Conclusions

In this paper we have presented a regime classification for the behavior of Pacific basin cyclones in

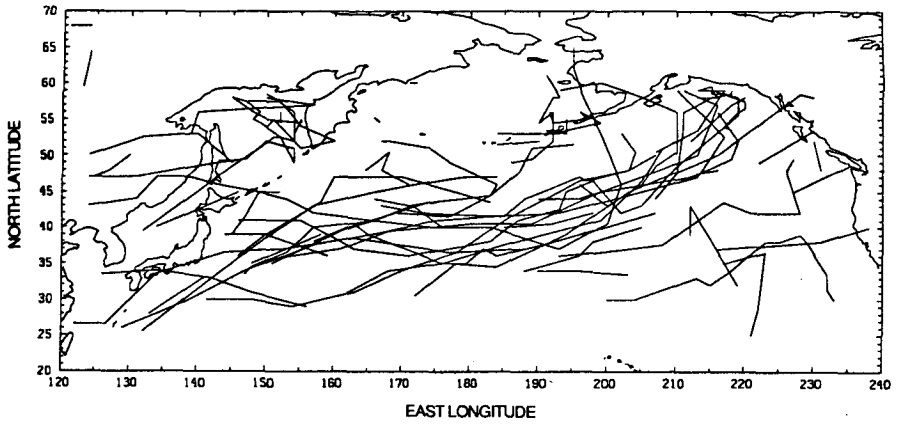

FIG. 11a. Cyclone tracks for 22 December 1982–20 January 1983: Type 3+ regime.

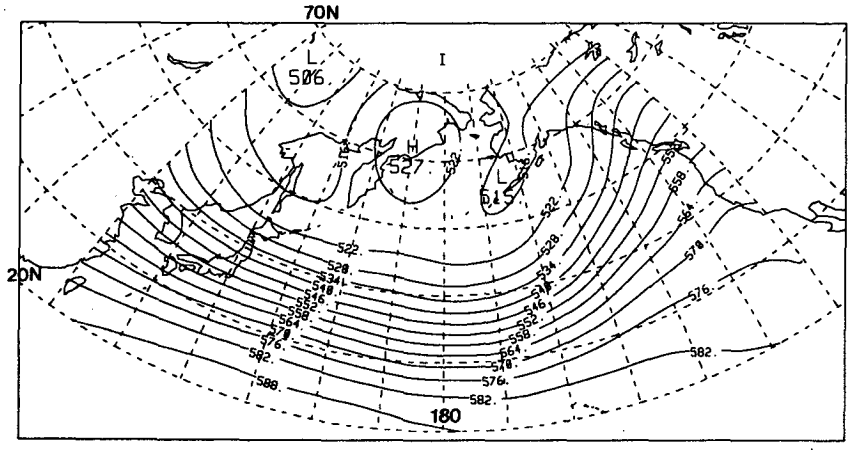

FIG. 11b. Composite field of 500 mb geopotential height for the period 22 December 1982–20 January 1983 at 1200 UTC: Type 3+ regime. The contour interval is 6 decameters.

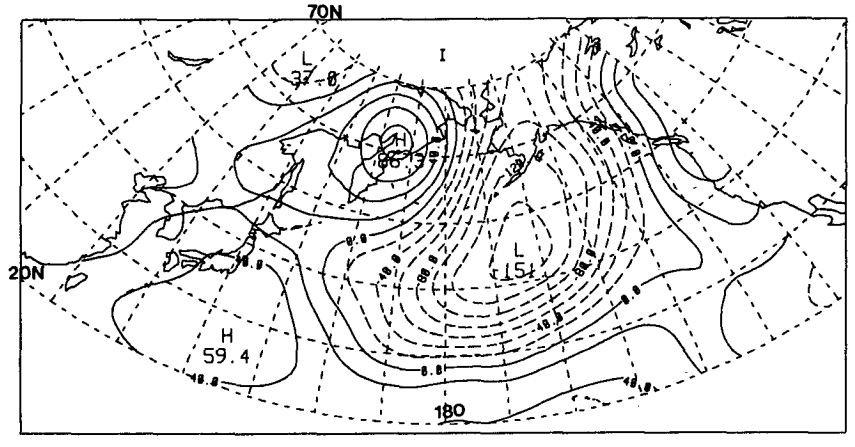

FIG. 11c. Composite field of 500 mb geopotential height anomalies for the period 22 December 1982–20 January 1983 at 1200 UTC: Type 3+ regime.

terms of a time rotated EOF analysis. A striking feature of our analysis is that the first three rotated factors explain very similar amounts of variance giving rise to six regimes which appear to be of near equal importance in terms of their influence on Pacific storm tracks. It should be pointed out the finding of six regime classes may be due in part to our analysis technique, and a more efficient, perhaps nonlinear, scheme might be able

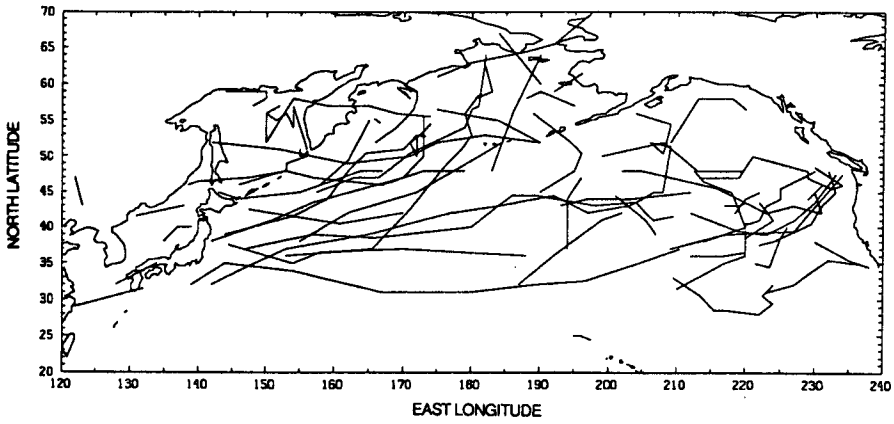

FIG. 12a. Cyclone tracks for 19 December 1977–17 January 1978: Type 3– regime.

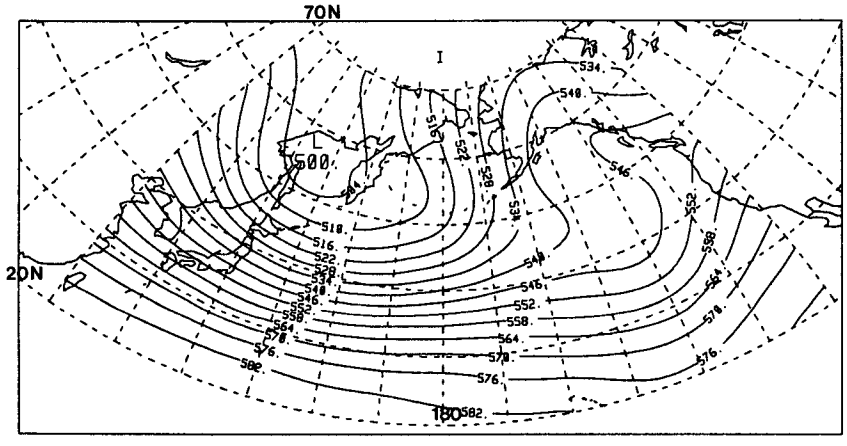

FIG. 12b. Composite field of 500 mb geopotential height for the period 19 December 1977–17 January 1978 at 1200 UTC: Type 3– regime. The contour interval is 6 decameters.

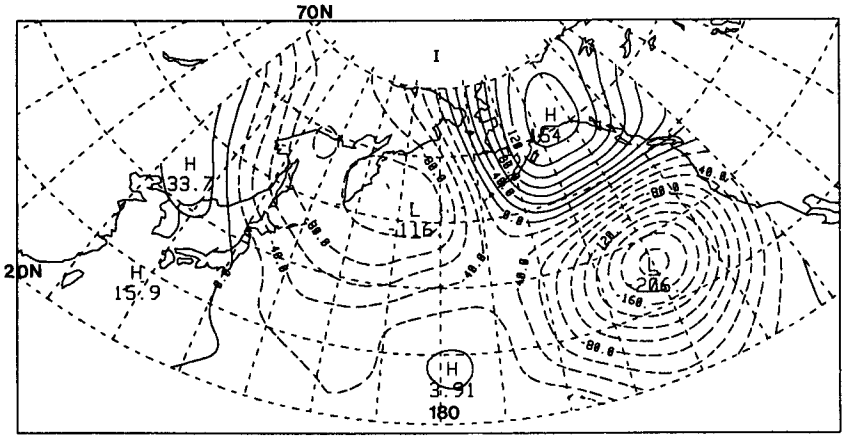

FIG. 12c. Composite field of 500 mb geopotential height anomalies for the period 19 December 1977–17 January 1978 at 1200 UTC: Type 3– regime.

to represent the variability in four or five classes; however, we have not been able to accomplish this and it seems unlikely that a classification into less than four regimes could succeed. This contrasts with our original intuitive feeling that Pacific flows might be characterized as one basic "zonal index" type variable that would

discriminate between "blocked" and "zonal" regimes. It seems that once again the real atmosphere strives to avoid simple classifications.

The low frequency interannual variability is no less confusing. For example, the moderate 1976–77 ENSO event is associated with a strong positive signal in rotated EOF 1; however, the 1980/81 winter is associated with an equally strong signal. The strong 1982–83 ENSO event is nearly normal in the EOF 1 time series, but is strongly positive in the EOF 2 series. In fact, the strongest annual mean anomalies of all are the positive EOF 3 signal in 1975/76 and the negative EOF 1 signal in 1981/82; years that are not generally associated with strong tropical circulation anomalies. In general, we interpret this lack of an obvious ENSO correlation as supportive of the idea that much of the observed midlatitude interannual variance is generated internally without recourse to tropical forcing. We are currently studying the relationships between cyclone tracks and tropical variables on shorter time scales. Early results of this work indicate that the rotated EOF 1 time series may be strongly linked with the tropical intraseasonal (40–50 day) oscillation.

Finally, we would like to comment on the relationship between our results and the results of Lau (1988), who has performed a study with similar objectives using a different methodology. Lau has performed an EOF analysis based on monthly mean rms amplitude of 2.5–6 day period band-pass 500 mb heights. This study differs from ours in two major respects: The first is the use of the band pass variance fields as a proxy for the cyclone tracks. The relationship between this quantity and the tracks was recently examined by Wallace et al. (1988). They found the relationship exhibited positional biases from synoptically determined cyclone tracks, although they observed no major changes in overall structure. Second, the use of monthly mean values in the Lau study is probably not the optimum choice for blocking time scales, since many blocking events do not last for 30 days and most of those that do may not be lined up on a calendar month boundary.

The differences between our analysis and the Lau results are substantial. His first Pacific EOF exhibits a monopole structure with a maximum near the date line, whereas our first pattern indicates much more of the shift of storm track density between the central part of the basin and the borders associated with central Pacific ridging. This differentiation is even more apparent in our rotated EOF 1 than it is in the unrotated field. His second EOF is a north–south dipole similar in general appearance to our rotated EOF 2, although it is displaced significantly southward and eastward from our EOF 2 and does not seem to be capable of describing behavior such as the 28 November–27 December 1978 case. The Pacific EOF 3 in the Lau analysis is similar to our unrotated EOF 3. Because of the findings of Wallace et al. (1988) we are inclined to view the differences between our results and the Lau results to be mainly due to the differences in the time resolution between the two studies, although our use of actual cyclone positions must also contribute.

In summary, we believe that the results of this analysis provide a concise way of describing changes in the cyclone climate of the Pacific basin. Through the examination of extreme periods we have verified that our rotated EOF extreme patterns do appear as regimes in the cyclone behavior and the good agreement with the 500 mb fields supports the dataset. The results of this analysis raise the obvious questions regarding possible forcings of these regime behaviors and connections with other parts of the planetary circulation which we plan to explore in future work.

Acknowledgments. This work has been supported by the National Science Foundation under Grants ATM-8516263, ATM-8746521, and ATM-8814816, the Atmospheric Environment Service, and the Natural Sciences and Engineering Research Council of Canada under operating Grant P0037433. We would like to thank Mr. Michel Nadeau and Mr. Timothy Bullock for their assistance in the compilation and presentation of data used in this study. Ms. Jodi Saeland provided valuable assistance with the figures and manuscript.

REFERENCES

Cureton, E. E., and R. B. D'Agostino, 1983: *Factor Analysis, An Applied Approach.* Lawrence Elburn, 457 pp.

Dole, R. M., 1986: Persistent anomalies of the extratropical Northern Hemisphere wintertime circulation: structure. *Mon. Wea. Rev.*, **114,** 1567–1586.

Elliot, R. D., 1949: A study of the effects of large blocking highs on the general circulation in the Northern Hemisphere westerlies. *J. Meteor.*, **6,** 67–85.

Gyakum, J. R., J. R. Anderson, R. H. Grumm and E. L. Gruner, 1989: North Pacific cold-season cyclone activity: 1975 through 1983. *Mon. Wea. Rev.*, **117,** 1141–1155.

Horel, J. D., 1981: A rotated principal component analysis of the interannual variation of the Northern Hemisphere 500 mb height field. *Mon. Wea. Rev.*, **109,** 2080–2092.

Lau, N.-C., 1988: Variability of observed midlatitude storm tracks in relation to low-frequency changes in the circulation pattern. *J. Atmos. Sci.*, **45,** 2718–2743.

Mass, C. F., H. J. Edmon, H. J. Friedman, N. R. Chaney and E. E. Recker, 1987: The use of compact discs for the storage of large meteorological and oceanographic data sets. *Bull. Amer. Meteor. Soc.*, **68,** 1556–1558.

Namias, J. and P. F. Clapp, 1949: Confluence theory of the high troposphere jet stream. *J. Meteor.*, **6,** 330–336.

O'Lenic, E. A., and R. E. Livezey, 1988: Practical considerations in the use of rotated principal component analysis in diagnostic studies of upper-air height fields. *Mon. Wea. Rev.*, **116,** 1682–1689.

Rex, D. F., 1950: Blocking action in the middle troposphere. *Tellus.*, **2,** 196–211.

Richman, M. B., and P. J. Lamb, 1985: Climate pattern analysis of three and seven day summer rainfall in the central United States: Some methodological considerations and a regionalization. *J. Climate Appl. Meteor.*, **24,** 1325–1343.

Wallace, J. M., G.-H. Lim and M. L. Blackmon, 1988: On the relationship between cyclone tracks, anticyclone tracks and baroclinic waveguides. *J. Atmos. Sci.*, **45,** 439–462.

White, W. B., and D. E. Clark, 1975: On the development of blocking ridge activity over the central North Pacific. *J. Atmos. Sci.*, **32,** 489–502.